Integration of Organic FETs With Organic Photodiodes for a Large Area, Flexible, and Lightweight Sheet Image Scanners

Takao Someya, *Member, IEEE*, Yusaku Kato, *Student Member, IEEE*, Shingo Iba, Yoshiaki Noguchi, Tsuyoshi Sekitani, Hiroshi Kawaguchi *Member, IEEE*, and Takayasu Sakurai, *Fellow, IEEE*

Abstract—A large-area, flexible, and lightweight sheet image scanner has been successfully manufactured on a plastic film by integrating high-quality organic transistors and organic photodetectors. The effective sensing area of the integrated device is 5×5 cm^2; the resolution, 36 dots per inch (dpi); and the total number of sensor cells, 5184. The pentacene transistors with top contact geometry have a channel length of 18 μm and mobility of 0.7 cm^2/Vs. Organic photodetectors composed of copper phthalocyanine and 3,4,9,10-perylene-tetracarboxylic-diimide distinguish between black and white parts on paper based on the difference in their reflectivity. Since this new area-type image-capturing device does not require any optics or mechanical scanning devices, the present sheet image scanners are mechanically flexible, lightweight, shock resistant, and potentially inexpensive to manufacture; therefore, they are suitable for human-friendly mobile electronics.

Index Terms—Flexible sensor, image sensor, large-area electronics, organic transistor.

I. INTRODUCTION

ORGANIC field-effect transistor (FET) integrated circuits [1]–[6] have attracted considerable attention since they have many attributes complementary to silicon very large-scale integrated systems (VLSIs) that yield high performance, but are expensive. The manufacturing costs of organic transistor circuits are expected to be lower even for a large area if they are fabricated using printing technologies and/or the roll-to-roll process. Furthermore, organic transistors are mechanically flexible [7], thin, lightweight, and shock resistant since the organic devices are manufactured on plastic films at low (ambient) temperature.

Recent studies on organic transistors are motivated by two major types of applications. One includes flexible displays such as paper-like displays or e-paper, where electric inks, electroluminescent (EL) devices, liquid crystals, or other mediums are powered by organic transistor active matrixes [4], [8]. The other type includes radio frequency identification tags [9], [10]. The printable features [11]–[13] of organic transistors are expected to be suitable for the implementation of integrated circuits in the field of packaging.

We recently demonstrated another promising application, that is, a large-area, flexible sensor. The first example of organic transistor-based large-area sensors is a pressure sensor matrix. Organic transistor active matrixes are used to read out pressure data from sensors. The new pressure sensor could be ideal for electronic artificial skin applications for future generations of robots [14]–[18]. Although it is well known that the mobility of organic semiconductors is about two or three orders of magnitude lower than that of poly- and single-crystalline silicon, the lower speed is tolerable for most applications of large-area sensors. For artificial skin in particular, the integration of pressure sensors and organic peripheral electronics enables us to take advantage of many benefits of organic transistors such as mechanical flexibility, large area, low cost, and relative ease of fabrication without suffering from their drawbacks.

In another new development in the field of large-area electronics, we have recently successfully demonstrated the large-area, flexible, and lightweight sheet image scanner based on organic semiconductors [19], [20]. In this paper, we report the technical details of sheet image scanners, particularly, the principle of imaging, manufacturing process, and electronic performance of individual sensor cells. The device is manufactured on plastic films by integrating organic FETs and organic photodiodes. Organic photodetectors distinguish between black and white parts on paper based on the difference in their reflectivity. The effective sensing area of the integrated device is 5×5 cm^2; resolution, 36 dpi; and the total number of sensor cells, 5184. The pentacene FETs with top contact geometry have a channel length of 18 μm and a mobility of 0.7 cm^2/Vs. The total thickness and the weight of the entire device are 0.4 mm and 1 g, respectively. Furthermore, we have successfully obtained the images of several characters whose size is approximately 1×1 mm^2 by using two-dimensional (2–D) arrays of a photodiode matrix without organic transistors. The present sheet image scanners are mechanically flexible, lightweight, very thin and, therefore, suitable for human-friendly mobile electronics.

II. MANUFACTURING PROCESS

As may be observed from Fig. 1, the integrated device formed on a plastic film is mechanically flexible, very thin, and lightweight. The image of the chip and a circuit diagram of the core section are shown in Fig. 2(a) and (b), respectively. Fig. 3 contains a schematic
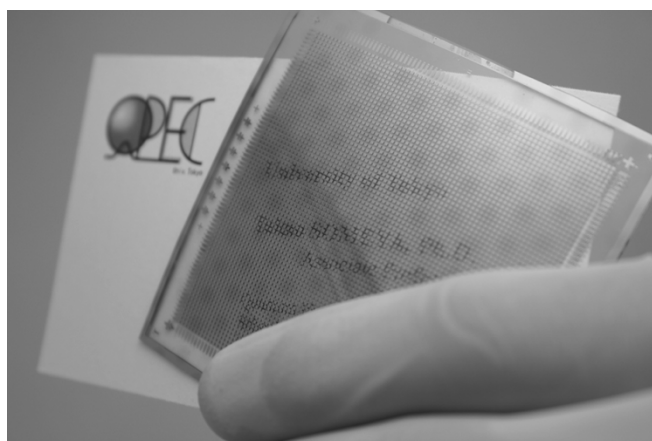
Fig. 1. Image of a large area, flexible, and lightweight sheet-type image scanner placed onto the business card for capturing images. The effective scanning size is 50×50 mm^2 and the resolution, 36 dpi.
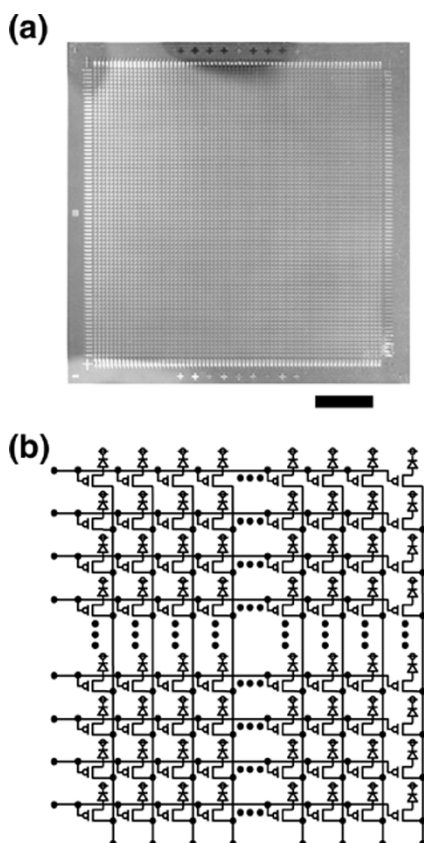

Fig. 2. (a) Image and (b) a circuit diagram of the present sheet-type image scanner consisting of organic transistors integrated with organic photodiodes. Scale bar is 1 cm.

illustration of the device structure along with the chemical structure of each layer. The organic FET matrix and the photodiode matrix have been manufactured separately on different plastic films in a clean room (class 100–1,000) and then laminated with each other using a silver paste patterned by a microdispenser. Alternatively, we used anisotropic conductive films (Anisolm, Hitachi Chemical Company Ltd., Japan) for the lamination process.

First, a 72×72 ($\sim 5,184$) matrix of pentacene FETs with top contact geometry is manufactured with an ultrafine shadow mask (Athene Company, Ltd., Japan). The base film (substrate) is a transparent poly(ethylene naphthalate) (PEN) film (Teonex
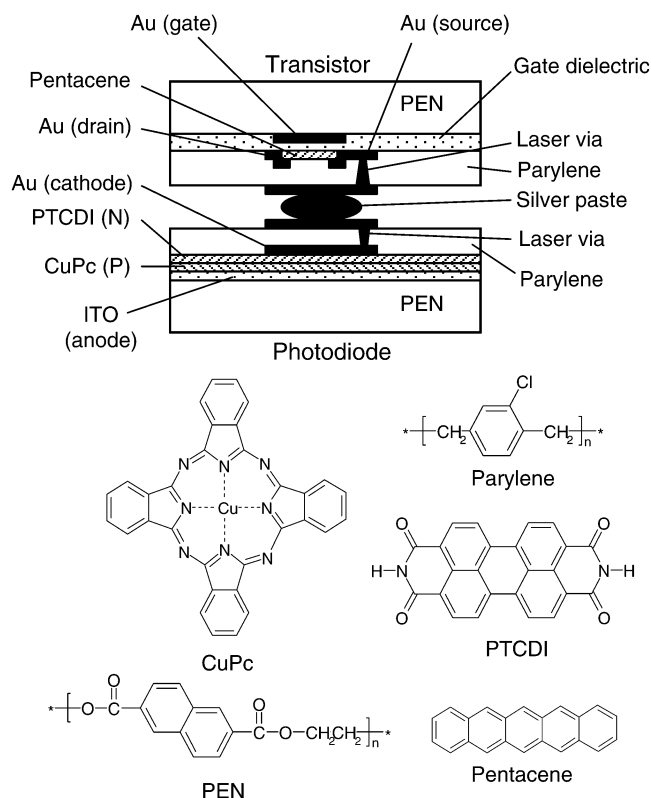

Fig. 3. Cross-sectional illustration of the present device consisting of a organic transistor and organic pn-junction diode. The chemical structure of each organic layer is also shown.

Q65, Teijin Dupont Films, Japan) with a thickness of 125 μm.[1] Before the manufacturing process, the base film is heated at 190 °C for 1 h. This prebake process plays a very important role in minimizing the shrinkage of the film during the cross-linking of polyimide gate dielectric layers, which occurs at 180 °C. The surface of the base film is coated with a 150-nm-thick gold layer with a 5-nm-thick chromium adhesion layer in a vacuum evaporator with shadow masks to form a gate electrode. The polyimide precursors (Kemitite CT4112, Kyocera Chemical Company, Ltd., Japan) are then spin-coated and cured at 180 °C to form 630-nm-thick gate dielectric layers [21]. A 50-nm-thick pentacene is deposited to form a channel layer. The pentacene [22], [23], purchased from Aldrich, is purified in the home-made zone-sublimation system within a mixture of H$_2$ and N$_2$ gases. A 60-nm-thick gold layer is evaporated through shadow masks to form the source and drain electrodes of the transistors. Fig. 4(a) shows the magnified image of four transistors before integrating with organic diodes. The channel length L and width W are 18 μm and 400 μm, respectively. The periodicity is 700 μm, which corresponds to a resolution of 36 dpi.

The photodiodes are separately manufactured on the different films. The base film of photodiodes is a PEN film coated with ITO with a sheet-resistance of 95 $\Omega/\square$. The surface of ITO coated films is cleaned with an organic solvent and, subsequently, a UV-ozone cleaner. A 30-nm-thick p-type semiconductor of copper phthalocyanine (CuPc) and a 50-nm-thick n-type

---

[1]The optical transparency of PEN is as high as 87% in the visible wavelength according to the vendors information. Such a high transparency of a base film is very important to obtain high-quality images, since optical absorption and/of optical scattering might degrade the contrast of images.
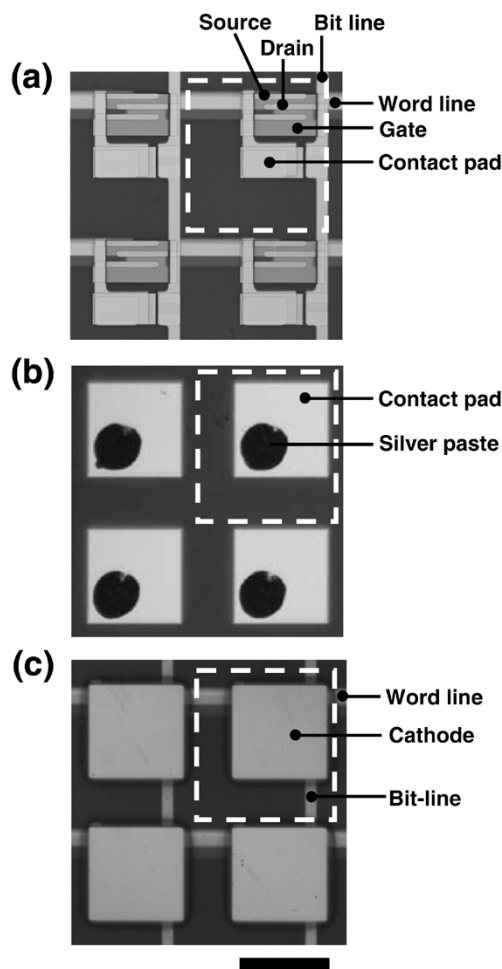
Fig. 4. (a) Magnified image of four transistors before integrating with organic diodes. (b) A magnified image of four contact pads with silver paste islands before laminating organic transistor films and organic diode films. (c) A magnified image of four sensor cells integrating organic transistors and organic photodiodes. The entire transistor regions are covered by the photodiodes. The channel length L and width W are 18 and 400 μm, respectively. As indicated by the dashed line, the periodicity is 700 μm.
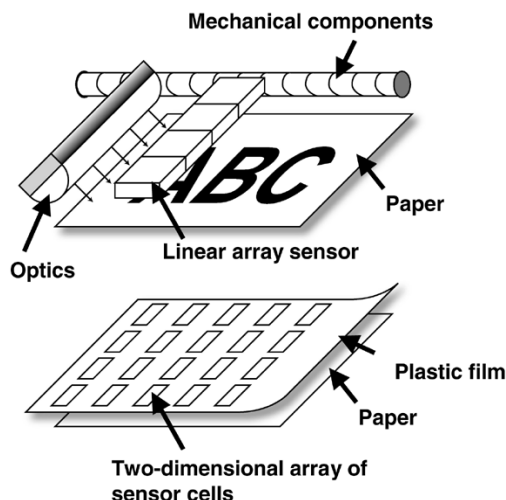

Fig. 5. Schematic illustration of a conventional scanner and the proposed sheet-type scanner. A conventional scanner consists of a linear array sensor, light source, and mechanical components. The new scanner consists of a 2-D array of organic photodiodes coupled with organic transistors, which can be read out electrically by the organic transistors.

semiconductor of 3,4,9,10-perylene-tetracarboxylic-diimide (PTCDI) are deposited in a vacuum sublimation system. Both materials are purified once in the sublimation system. The thickness of CuPc and PTCDI is one of the most important parameters to optimize the electronic performances and yields, as will be shown later in detail. Devices with different thicknesses are also fabricated for comparison. A 150-nm-thick gold layer was deposited as cathode electrodes. The optical transparency of the 150-nm-thick gold layer is small enough and this layer works as a light-shielding layer. Other metals are also used as cathode electrodes for comparison. We choose Au as the cathode electrode to manufacture the final structures because Au electrodes enable us to obtain a reliable interconnection by the laser via process. Although Au has a relatively large workfunction, the device exhibits a fairly reasonable electric performance as a photodetector, as will be shown later. The size of cathode electrodes and the periodicity of photodiodes used to integrate with organic transistors are 450×450 μm^2 and 700×700 μm^2, respectively; however, smaller photodiodes are also fabricated for comparison.

Both films with organic FETs and photodiodes are transferred to the vacuum chamber without exposing them to air after the

manufacturing process; further, they are uniformly coated by a 2-μm-thick poly-monochloro-para-xylylene (parylene) passivation layer. Parylene spots on electrodes are removed by a CO_2 laser drilling machine for electronic interconnections. It should be noted that in the structures of photodiodes, laser via interconnections have been directly made on gold cathode electrodes through parylene intermediate layers. Therefore, manufacturing good interconnections without causing electric short was a significant issue. We manufactured good interconnections with high yields by optimizing the thicknesses of gold electrodes and parylene layers, as will be described in detail later.

Please note in Fig. 3 that organic semiconductor layers of transistors are sandwiched between two electrodes: the gate electrode and the contact pad to integrated with sensors. Although organic transistors are photosensitive, the light-shielding layers cover the channel layers in the present design. As a result, effects of light on transistors are negligibly small.

Further, these films are laminated with each other. Silver paste islands were patterned by a microdispenser (Musashi Engineering Company, Ltd., Japan) for vertical interconnections. Alternatively, anisotropic conductive films (Anisolm, Hitachi Chemical Company, Ltd., Japan) are also used. Fig. 4(b) shows the magnified image of four contact pads with silver paste islands before the lamination of organic transistor and organic diode films. Fig. 4(c) shows the magnified image of four sensor cells integrating organic transistors and organic photodiodes. The entire transistor regions are covered by photodiodes.

III. PRINCIPLE OF IMAGING

Fig. 5 shows the difference between the conventional and present scanning method, which does not require any mechanical or optical component. In conventional scanners, a linear array sensor is moved from the top of a page to its bottom to capture images. The new design employs a 2-D array of organic photodiodes coupled with organic transistors. Instead of a mechanical scanning procedure, the signal of the photodiodes is read out electrically by the organic transistors, avoiding the need
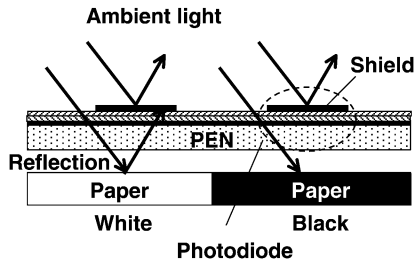
Fig. 6. Principle of imaging with the proposed sheet image scanner, which is placed on the paper with white and black regions.

to use any movable part. As a result, the device is thin, light-weight, and mechanically flexible.

The principle of imaging with the present sheet image scanner can be described as follows. As can be observed from Fig. 6, if all incident light directly reaches the active layers, photodetectors cannot distinguish between black and white. Therefore, we prepared light-shielding layers to prevent photodetectors from being exposed to direct incident light. Direct light cannot reach the active layers. In this case, the incident light passing though transparent regions is reflected on the white part of paper and reaches the active layers, while that on black does not reach the active layers. In this manner, the new scanner can distinguish between black and white.

Please note here that this principle does not rely on the size of the total sensing area. The size of the prototype is 5×5 cm^2. However, if the devices are manufactured by printing technologies, similar structures with a large effective sensing area will be feasible and those can be functional in the same principle.

IV. ELECTRIC CHARACTERISTICS

In this section, we present a detailed report on the electronic performance of stand-alone organic transistors, photodiodes, and integrated devices, which are characterized under an ambient environment with adequate device sealing or a nitrogen environment without sealing.

A. Organic Photodiodes

1) Photo-Response of Organic pn-Diodes: Fig. 7 shows the typical current–voltage (I–V) characteristic of the manufactured organic photodiodes with 450×450 μm^2 gold cathode electrodes under illumination of light with different light intensities. The light source is a halogen lamp with a cold filter. The light intensity is changed from 0 to 175 mW/cm^2. In the case of no light illumination, the threshold voltage of forward-biased photodiodes is 4 V, while the breakdown voltage is -17 V. The density of the photocurrent with a reverse bias of -4 V as a function of the light intensity is plotted in Fig. 7(b). The current is proportional to a light intensity of up to 100 mW/cm^2, showing good linearity of photoresponses as sensors.

2) Single-Layer Structures: For the purpose of comparison, we also processed two structures with single 80-nm-thick organic semiconductor layers—CuPc and PTCDI layers. In both cases, these individual layers are sandwiched between ITO and Au electrodes. Fig. 8(a) and (b) shows the current-voltage characteristics of the structure with a single CuPc layer and that with PTCDI, respectively. The light illumination was performed in the same
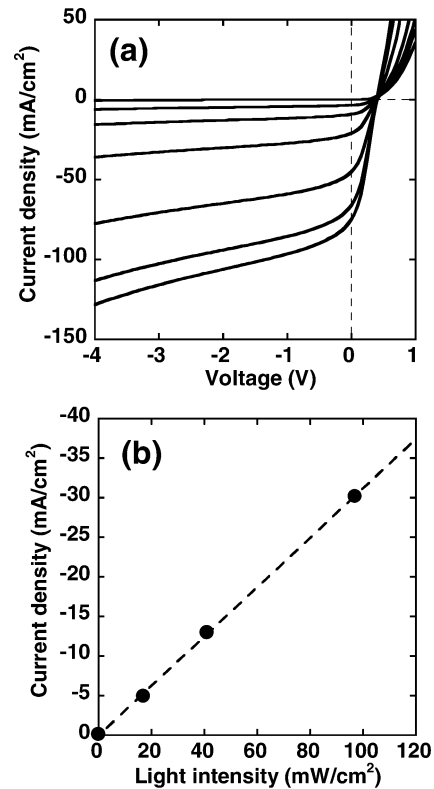

Fig. 7. (a) Typical I–V characteristic of the manufactured organic photodiodes with 450×450 μm^2 gold cathode electrodes under illumination of light with different intensities. The light intensities are 0, 20, 40, 100, 140, 170, and 180 mW/cm^2. (b) Photocurrent density with a reverse bias of -4 V is plotted as a function of the light intensity.

manner as mentioned above. Although both the single-layer devices exhibit fairly large responses to light, the I–V curves of the two devices do not exhibit saturation. When the photodetectors are integrated with transistors, the shapes of the I–V curves play a very significant role in enhancing the photoresponse of the integrated devices. As will be shown later in detail, the I–V curves exhibiting saturation exhibit a large photoresponse for the integrated devices; therefore, we have used double layer structures consisting of CuPc and a PTCDI layers in the final structures.

3) The Thickness of Organic Semiconductors: In order to obtain a large photoresponse, we have altered the total thickness of the organic layers of the organic diodes with gold cathode electrodes. The thicknesses of the CuPc and PTCDI layers are set to have a ratio of 3:5; for example, the thickness of CuPc and PTCDI are 30 and 50, or 60 and 100 nm, respectively. In other words, this is twice the total thickness of two organic layers. As shown in Fig. 9, we have measured the currents under the light intensity of an ambient atmosphere. Currents are measured at a forward voltage bias of 2 V as a function of the total thickness of organic layers. The photoresponse becomes larger with a reduction in the thickness of organic layers; this indicates that the photoresponse of the present devices is not limited by light absorption in organic layers, but by the transport of photogenerated carriers in organic layers. On the other hand, we have found that the yields of pn-diodes depend on the total thickness of organic layers—it decreases when thickness is reduced to less than 80 nm due to a short between the anode and cathode. In order to ensure high yields, we set the total thickness of organic layers as 80 nm.
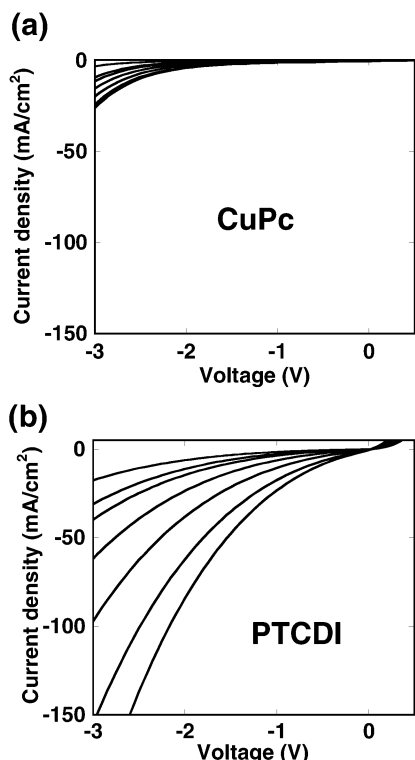
(a)

(b)

Fig. 8.   Photocurrent density of single organic layers of (a) a 80-nm-thick CuPc and (b) a 80-nm-thick PTCDI that is sandwiched between the ITO and Au electrode as a function of light intensity at 0, 20, 40, 100, 140, 170, and 180 mW/cm^2. The size of Au electrode is 450×450 μm^2.
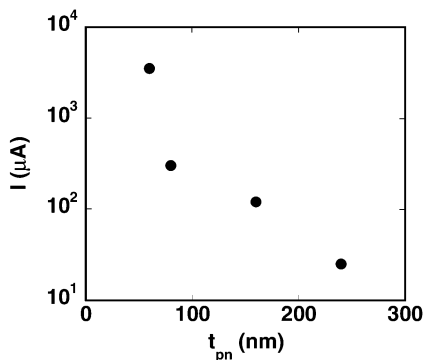

Fig. 9.   Photocurrents at a forward voltage bias of 2 V are plotted as a function of the total thickness of organic layers.

4) Measurement in the Reflection Geometry: As shown in Fig. 10, the present device distinguishes between black and white in the reflection geometry. One of the organic photodetectors is positioned on a sheet of white paper that contains a black region printed by a laser printer. The device is uniformly illuminated from the top surface with a light intensity of 40 mW/cm^2. Fig. 10 shows the I–V curves measured on white and black parts; a photocurrent ratio of 8:1 is obtained at a voltage bias of -4 V. This ratio is exactly the same as white-to-black reflectivity ratio of paper.

5) Anode Electrodes: We use as anode electrodes an ITO layer prepared on PEN films by a sputtering machine. The sheet-resistance and surface smoothness of ITO layers are crucial factors. The sheet-resistance of the present ITO layers is 95 $\Omega/\square$. In the device with ITO of a higher sheet-resistance, the current is limited by the sheet-resistance of ITO rather than that of the
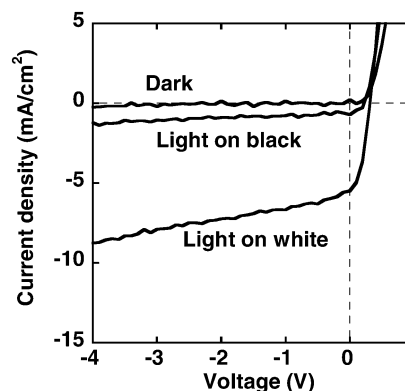

Fig. 10. I–V characteristics of a 36 dpi-photodiode array without transistors are measured with and without light on black and white regions.
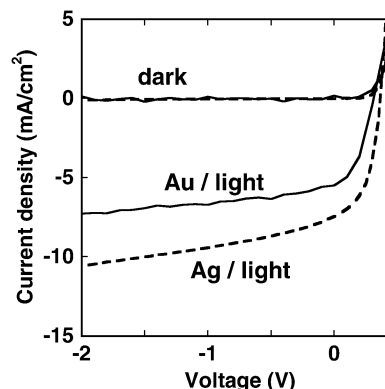

Fig. 11. I–V curves of the device with silver and gold cathode electrodes under illumination of light with a biased voltage of -2 V are plotted as dashed and solid lines, respectively. The current density of photodiodes placed on the white paper is measured with and without light.

organic layers. Thus, the change in current induced by light is revealed by the sheet-resistance of ITO. A smooth surface ITO is crucial since it has a great influence on the yields and photoresponse of organic diodes. When we characterized the surfaces of ITO by AFM, the root-mean-square (RMS) for ITO was 0.6–0.9 nm. Since there occurs a tradeoff between surface smoothness and sheet-resistance of ITO, it is important to use ITO that is optimized for photodiode applications.

6) Cathode Electrodes: Although gold has a relatively high workfunction, the device with gold cathode electrodes exhibits a fairly large photoresponse, as mentioned above. This experimental result is reasonable since electrons are not injected, but extracted from the gold electrodes for the photodiodes under negative voltage bias. We have also fabricated the photodiode structures with silver cathode electrodes, which have a smaller workfunction than gold. Fig. 11 shows the I–V curves of the device with a silver cathode electrode under illumination of light. The magnitude of photocurrents in devices with gold is slightly less than devices with silver. This difference can be ascribed to the difference of workfunction between gold and silver and/or the difference of evaporation temperature between gold and silver; the higher evaporation temperature may cause thermal damage to organic semiconductor. Both devices can be manufactured with high yields, i.e., exceeding 99%.

7) Laser via Interconnects: We selected gold electrodes as cathodes because only gold electrodes enable us to achieve high
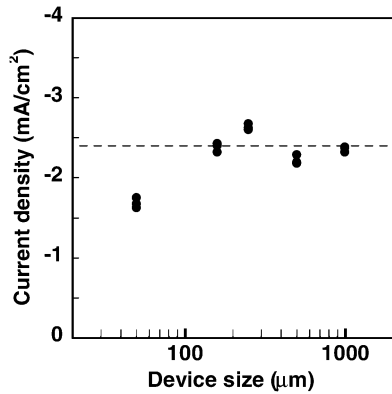
Fig. 12.   Photocurrent density of the pn-photodiode with various sizes of gold cathode electrodes from 1×1 mm^2 to 50×50 μm^2. Measurements are performed under illumination of light of 70 mW/cm^2.

yields for the laser via interconnection. We examined the yields for the laser via interconnection by changing the total thickness of organic layers, gold cathode electrodes, and parylene layers. The output power of a laser drill machine is changed from 12 to 24 mJ in steps of 0.6 mJ to investigate the optimized conditions for each structure. We have found that the yields for the laser via process are very sensitive to the thickness of the gold layers. In case that the thickness of the cathode electrode is more than 300 nm, all the interconnections result in short or open for all light intensity of CO$_2$ laser. On the other hand, in case of a cathode electrode with a thickness of less than 300 nm, all the interconnections are short for a light intensity exceeding 16.8 mJ and open below 15.6 mJ. In contrast, the yields of the via process are not sensitive to the thickness of the parylene layer. When the thickness of parylene is set to be from 2 μm to 5 μm, more than 19 out of 20 devices exhibit good via interconnections. Although we have attempted to conduct a similar process using silver cathode electrodes, we were unable to find an appropriate condition for the laser via process—a laser light with an intensity of 0.9 mJ or above causes a short.

8) Reduction of Device Dimensions: The reduction of device dimensions is crucial for increasing the spatial resolution of image scanners. We have prepared photodiodes by using various sizes of gold cathode electrodes from 1×1 mm^2 to 50×50 μm^2. The photocurrent density is measured under illumination of light (70 mW/cm^2) as shown in Fig. 12. When the device dimensions are reduced to 50×50 μm^2, the photocurrent density decreases by only 25%, which is sufficient to achieve a spatial resolution of 250 dpi.

B. Organic FETs

Fig. 13 shows the typical characteristics of the manufactured p-type organic transistor. The measured mobility is as high as 0.7 cm^2/Vs. The entire device failure can be attributed to gate leakage. The initial yield strongly depends on the thickness of polyimide gate dielectric layers. When polyimide precursors of CT4112 are spin-coated at a revolution rate of 4500 rpm without dilution, the thickness of the polyimide layers becomes 630 nm after the curing process. For the devices with 630-nm-thick polyimide gate dielectric layers, the initial yield exceeds 99%. We can easily reduce the thickness of gate dielectric layers if we
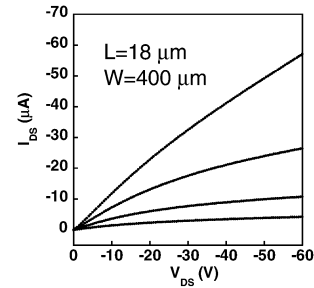
Fig. 13.   Typical characteristics of the manufactured p-type organic transistor. A source-drain current (I_{DS}) is shown as a function of source-drain voltage (V_{DS}) swept from 0 to -60 V. A gate voltage (V_{GS}) is varied from 0 to -60 V in steps of -10 V.
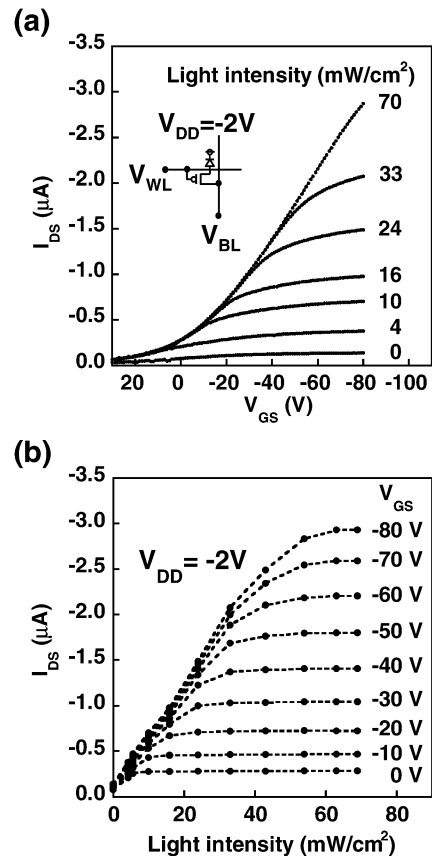
Fig. 14.   Electric performance of one sensor cell of the 36-dpi integrated device. The power supply V_{DD} is -2 V. (a) I_{DS} versus V_{GS} under various intensities of light. (b) I_{DS} versus light intensity with a different V_{GS} bias.

dilute the source materials (Kemitite CT960, Kyocera Chemical Company, Ltd., Japan) composed of n-methyl-2-pyrrolidone (NMP) and/or increase revolution rate during spin coating. The yields gain importance with an increase in the number of sensor cells. This aspect will be discussed at a later point.

C. Integrated Device

One of the sensor cells consisting of one transistor and photodetector is measured under illumination of various intensities of light up to 70 mW/cm^2. Fig. 14 shows the typical I–V characteristics of the sensor cell. Fig. 14(a) shows I_{DS} as a function of V_{GS}, while Fig. 14(b) shows I_{DS} retraced as a function of light intensity. When $V_{GS} = -80$ V is applied, I_{DS} is proportional to a light intensity of up to 40 mW/cm^2 and then saturates
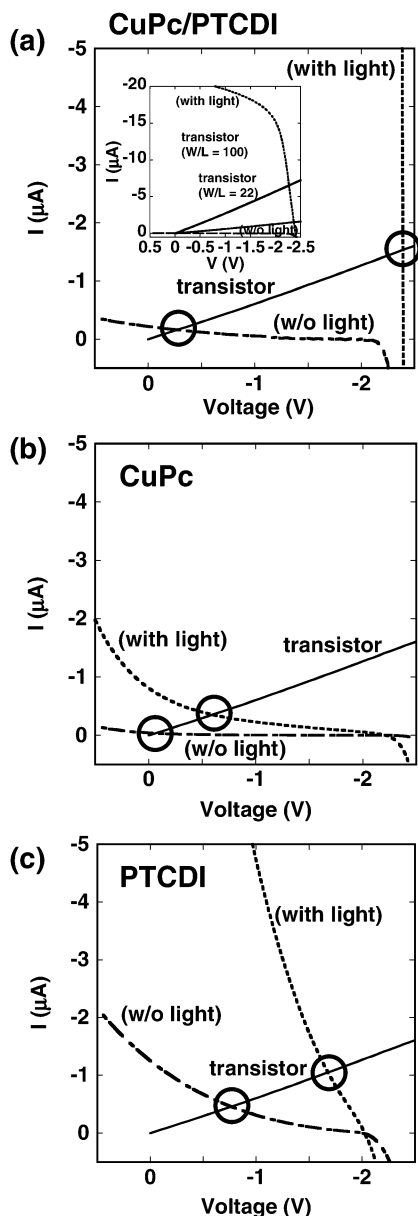
Fig. 15. I–V characteristics of photodetectors consisting of a (a) double layer structure of pn-diode and single layer structure of (b) CuPc and (c) PTCDI, with and without light, with the application of $V_{DD} = -5$ V. The dashed line represents I–V curves under light illumination (on) and the dashed-dotted line under dark (off). I–V characteristics of organic transistors with $W/L = 100$ and 22 are also measured at V_{DS} swept from 0 to -5 V.
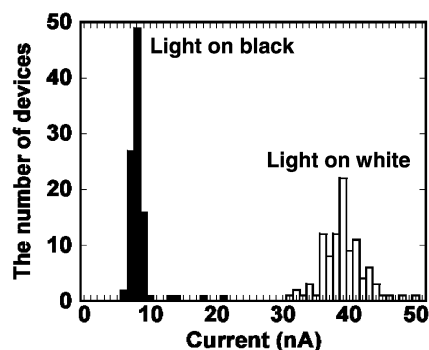

Fig. 16. Dispersion of hundred devices of the 250-dpi organic photodiode matrix without transistors. The effective size of each photodiode is 50×50 μm^2.

of power supply V_{DD} to be -5 V. The dashed line represents the data of photodetectors with light, while the dashed-dotted line represents data without light. The data of transistors with W/L= 22 are shown using black solid lines. The intersection points marked by solid circles indicate the current levels with and without light irradiation. These three figures clearly indicate that the slope of I–V curves of photodiodes must be abrupt near the origin of the coordinate axes. As shown in Fig. 15(a), large contrast ratios are obtained for double layer structures. The I–V curves for single layers of CuPc and PTCDI are shown in Fig. 15(b) and (c), respectively, showing that the contrast ratios are only 1.4 and 1.6, respectively, where FET has a W/L of 22 with an application of $V_{DD} = -5$ V. Photocurrents of a single organic layer—CuPc and PTCDI—do not exhibit steep rising characteristics and saturation, resulting in a small contrast. Thus, it is crucial to use double layer structures comprising p-type and n-type semiconductors, although single layer structures also function as photodetectors.

D. Imaging

We prepared a 250-dpi 10×10 organic photodiode matrix without organic transistors. The effective sensing area of each sensor cell is 50×50 μm^2, while the periodicity is 100 μm. The dispersion of the photocurrent of photodiodes with illumination of light (80 mW/cm^2) is shown in Fig. 16 under light illumination on black and white areas. Although a fairly large distribution of photocurrents is observed, performance distribution can be compensated by adequate calibration for each sensor cell. Such a situation is very different from the display application, which requires very high uniformity of each pixel.

We have positioned a sheet of paper with white capital letters "U," "O," and a square printed on it by a laser printer underneath the photodiode matrix and measured the photocurrent of each detector with light illumination (80 mW/cm^2). The mappings of photocurrents are shown in Fig. 17.

Although those are black-and-white images, it is not difficult to modify the present scanner so that it might capture a color image. Similar to conventional scanners, the straightforward method is to simply integrate the scanners with color filters.

V. Discussion

We would also like to address the following three issues. The first issue is that of reliability and stability of organic transis-

around a light intensity of 60 mW/cm^2, as shown in (b). In principle, the contrast ratio between black and white doesn't depend on light intensity if it is less than 40 mW/cm^2. However, the lowering light intensity decreases the photocurrent, resulting in degradation of the signal-to-noise ratio. Therefore, in order to obtain a high contrast ratio between black and white with high signal-to-noise ratio, it is appropriate to set the light intensity for white to be approximately 40 mW/cm^2.

At this point, it should be noted that the shape of the I–V curves of photodetectors play a very important role in obtaining a high contrast ratio between black and white. In order to estimate the contrast ratio from the data of the I–V characteristics of photodetectors and transistors, we retrace the experimental data as shown in Fig. 15, where we assume the voltage
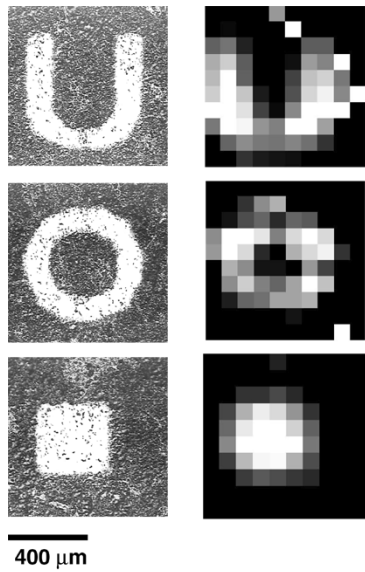
Fig. 17. White capital letters "U," "O," and a square printed by a laser printer on a paper (a) are placed on the 250-dpi organic photodetector matrix without organic transistors. The photocurrent of each detector is measured under light (80 mW/cm^2). The mapping of normalized photocurrents is compared with an image taken by a commercial 250-dpi scanner. The size of each image is 0.8×0.8 mm^2.

tors and diodes. In reality, the performance of our un-encapsulated device changes over a couple of days. This can be considered as the most stringent problem related to organic FETs, but it should be overcome by introducing adequate encapsulations that are similar to those for electroluminescent devices. Even if the organic transistors can solve reliability issues, hybrid structures consisting of organic transistors and silicon VLSI should be important to control organic electronics; this is one of the important studies in the future.

The second issue is that of high operation voltage. Lowering the operation voltage is not very difficult and can be undertaken by introducing the thinner gate dielectric layer or the use of high-κ materials. Indeed, we have already manufactured similar organic FETs using 230-nm-thick gate dielectric layers with a mobility above 0.1 cm^2/Vs; these FETs can be operated at a voltage of less than 10 V. As mentioned above, the yield becomes smaller as the thickness of the gate dielectric layers is reduced. Since there is a tradeoff between the operation voltage and yields, the design of thickness of gate dielectric layers is crucial.

The third issue is spatial resolution. Although the present resolution is 36 dpi with organic transistors, almost all the practical applications require 250 dpi for the spatial resolution. We have confirmed that an organic photodiode array can distinguish between black and white in a reflection geometry up to 250 dpi; however, the bottleneck to laminate two films for integration with organic transistors exists in the via process. The diameter of via holes processed by a CO_2 laser drilling machine is typically 50–100 μm. However, we expect to reduce the size of via holes when we use lasers with shorter wavelengths such as excimer lasers or YAG lasers.

When the spatial resolution is improved and, subsequently, the total number of sensor cells is increased, it becomes one of the critical issues to obtain a higher on/off ratio, higher yields,

and shorter delays of readout time, which will be addressed hereafter separately.

A. Requirements for On/Off Ratio

It is very important to obtain a high on/off ratio for organic transistors. The photocurrent flowing through each bit line is the product of the number of transistors on each bit line and the off current that always flows through each bit line. In order to measure the mapping of photocurrents, the total amount of dark current must be less than the on current of one sensor cell. The typical on/off ratio of our transistors is 10^4–10^5, if the off current is defined as the minimum current at the positive voltage bias. We have recently found that the on/off ratio can be reduced drastically when the device is annealed at 140 °C under nitrogen atmosphere [24]. Further improvement of electronic performance will be feasible by using these annealed transistors.

B. Requirements for Quantum Efficiencies of Photodiodes

With an increase in the spatial resolution, the size of each photodetector becomes smaller and, consequently, the photocurrent of one sensor becomes smaller. For example, the photocurrent density of the present photodiodes was -14 mA/cm^2 under light illumination of 180 mW/cm^2 and the application of -4 V. This corresponds to -29 μA for the resolution of 36 dpi, while it becomes -2.5 μA for 300 dpi. In the reflection geometry under a light illumination of 180 mW/cm^2, the photocurrent density was decreased to -8.8 mA/cm^2, which corresponds to -18 μA for 36 dpi and -0.16 μA for 300 dpi when we apply a forward voltage bias of -4 V. The measurement of small currents requires an amplifier, which makes the readout circuit complicated and expensive. Thus, it is very important to increase the quantum efficiency or the photocurrents of photodiodes. The structures of photodiodes are fairly identical to those of organic solar cells. Recently developed technologies for organic solar cells are helpful in improving the electric performance of organic photodetectors.

C. Device Failure

There are various kinds of device failures associated with transistors, diodes, and via electric interconnects. An example of typical device failure of organic transistors is leakage through gate dielectric layers, referred to as gate leakage. Other major failures are shorts between the anode and cathode electrodes of organic diodes and bad electric interconnections through laser via. Among these typical failures, one of the most serious is that of gate leakage, which sometimes makes it impossible to measure all the other sensor cells connected to the same bit lines as the transistor with gate leakage. On the other hand, the short between diodes makes it impossible to distinguish between black and white since large currents due to the shorted diodes are always recognized as white; bad interconnections, as black. Device failures of these two types render only one sensor cell nonfunctional, although one transistor with gate leakage renders one line nonfunctional. Here, we wish to emphasize that some missing data points are acceptable for most of the sensor applications since these points can be interpolated by a software after the measurements have been taken.

D. Crosstalk

There are two possible factors that cause crosstalk in the present design. The one is a leakage current flowing through gate insulators of transistors. It is important to suppress the chance of a gate leakage. The other is an event that the light is scattered from the neighboring cells or others and reaches an active layer of a photodiode. This type of crosstalk can be minimized by reducing the spacing between the active layer and the target paper, i.e., by decreasing the thickness of the base film.

E. Readout Circuitry

Although the drawback of organic transistors is a slow speed, we have demonstrated that this problem can be overcome by using a circuit concept called "double word-line and bit-line structure" which reduces the time delay by a factor of 5 and the power consumption by a factor of 7. To manufacture a new circuit, two different films with organic transistors are stacked along with the photodetector film. The technical details can be seen in [20].

F. Unique Applications

The new scanner is thin, lightweight, and flexible. The total thickness of the device is approximately 0.4 mm and its weight is approximately 1 g. The present scanner is suitable for mobile electronics and can be easily carried in a pocket. The new scanner would have unique applications beyond the portability feature. For example, it can be bended such that it can entirely cover at once the folded page of a thick open book. It would be also suitable for the recording of fragile, historically invaluable documents. A label affixed to a bottle of wine could also be accurately and conveniently scanned.

VI. Conclusion

We have demonstrated a sheet image scanner integrating organic transistors and organic photo detectors. The device with light shielding layers can distinguish between black and white in the reflection geometry. Since the new image-capturing device does not have any optical or mechanical component, it is lightweight, shock resistant, flexible, and suitable for human-friendly mobile application because it can be rolled and carried in a pocket.

References

[1] B. Crone, A. Dodabalapur, Y.-Y. Lin, R. W. Filas, Z. Bao, A. LaDuca, R. Sarpeshkar, H. E. Katz, and W. Li, "Large-Scale complementary integrated circuits based on organic transistors," *Nature*, vol. 403, pp. 521–523, Feb. 2000.

[2] C. J. Drury, C. M. J. Mutsaers, C. M. Hart, M. Matters, and D. M. de Leeuw, "Low-Cost all-polymer integrated circuits," *Appl. Phys. Lett.*, vol. 73, pp. 108–110, Jul. 1998.

[3] G. H. Gelinck, T. C. T. Geuns, and D. M. de Leeuw, "High-Performance all-polymer integrated circuits," *Appl. Phys. Lett.*, vol. 77, pp. 1487–1489, Sep. 2000.

[4] G. H. Gelinck, H. E. A. Huitema, E. van Veenendaal, E. Cantatore, L. Schrijnemakers, J. B. P. H. van der Putten, T. C. T. Geuns, M. Beenhakkers, J. B. Giesbers, B. -H. Huisman, E. J. Meijer, E. M. Benito, F. J. Touwslager, A. W. Marsman, B. J. E. van Rens, and D. M. de Leeuw, "Flexible active-matrix displays and shift registers based on solution-processed organic transistors," *Nature Mater.*, vol. 3, pp. 106–110, Feb. 2004.

[5] R. Brederlow, S. Briole, H. Klauk, M. Halik, U. Zschieschang, G. Schmid, J.-M. Gorriz-Saez, C. Pacha, R. Thewes, and W. Weber, "Evaluation of the performance potential of organic TFT circuits," in *Proc. ISSCC*, Feb. 2003, pp. 378–379.

[6] E. Huitema, G. Gelinck, B. van der Putten, E. Cantatore, E. van Veenendaal, L. Schrijnemakers, B.-H. Huisman, and D. M. Leeuw, "Plastic transistors in active-matrix displays," in *Proc. ISSCC*, Feb. 2003, pp. 380–381.

[7] T. Sekitani, Y. Kato, S. Iba, H. Shinaoka, T. Someya, T. Sakurai, and S. Takagi, "Bending experiment on pentacene field-effect transistors on plastic films," *Appl. Phys. Lett.*, vol. 86, no. 073 511, Feb. 2005.

[8] J. A. Rogers, Z. Bao, K. Baldwin, A. Dodabalapur, B. Crone, V. R. Raju, V. Kuck, H. Katz, K. Amundson, J. Ewing, and P. Drzaic, "Paper-Like electronic displays: Large-area rubber-stamped plastic sheets of electronics and microencapsulated electrophoretic inks," *Proc. Nat. Acad. Sci.*, vol. 98, pp. 4835–4840, Apr. 2001.

[9] P. F. Baude, D. A. Ender, M. A. Haase, T. W. Kelley, D. V. Muyres, and S. D. Theiss, "Pentacene-Based radio-frequency identification circuitry," *Appl. Phys. Lett.*, vol. 82, pp. 3964–3966, Jun. 2003.

[10] P. F. Baude, D. A. Ender, T. W. Kelley, M. A. Haase, D. V. Muyres, and S. D. Theiss, "Organic semiconductor RFID transponders," in *IEDM Tech. Dig.*, Dec. 2003, pp. 191–194.

[11] H. Sirringhaus, T. Kawase, R. H. Friend, T. Shimoda, M. Inbasekaran, W. Wu, and E. P. Woo, "High-Resolution inkjet printing of all-polymer transistor circuits," *Science*, vol. 290, pp. 2123–2126, Dec. 2000.

[12] Y. -L. Loo, T. Someya, K. W. Baldwin, Z. Bao, P. Ho, A. Dodabalapur, H. E. Katz, and J. A. Rogers, "Soft, conformable electrical contacts for organic semiconductors: High-resolution plastic circuits by lamination," *Proc. Nat. Acad. Sci.*, vol. 99, pp. 10252–10 256, Aug. 2002.

[13] N. Stutzmann, R. H. Friend, and H. Sirringhaus, "Self-Aligned, vertical-channel, polymer field-effect transistors," *Science*, vol. 299, pp. 1881–1884, Mar. 2003.

[14] T. Someya, T. Sekitani, S. Iba, Y. Kato, H. Kawaguchi, and T. Sakurai, "A large-area, flexible pressure sensor matrix with organic field-effect transistors for artificial skin applications," *Proc. Nat. Acad. Sci.*, vol. 101, pp. 9966–9970, Jul. 2004.

[15] H. Kawaguchi, T. Someya, T. Sekitani, and T. Sakurai, "Cut-and-Paste customization of organic FET integrated circuit and its application to electronic artificial skin," *IEEE J. Solid-State Circuits*, vol. 40, no. 1, pp. 177–185, Jan. 2005.

[16] T. Someya, H. Kawaguchi, and T. Sakurai, "Cut-and-Paste organic FET customized ICs for application to artificial skin," in *Proc. ISSCC*, Feb. 2004, pp. 288–289.

[17] T. Someya and T. Sakurai, "Integration of organic field-effect transistors and rubbery pressure sensors for artificial skin applications," in *IEDM Tech. Dig.*, Dec. 2003, pp. 203–206.

[18] T. Someya *et al.*, "Conformable, flexible, large-area networks of pressure and thermal sensors with organic transistor active matrixes," *Proc. Nat. Acad. Sci.*, vol. 102, no. 8, pp. 12321–12325, Aug. 2005.

[19] T. Someya, S. Iba, Y. Kato, T. Sekitani, Y. Noguchi, Y. Murase, H. Kawaguchi, and T. Sakurai, "A large-area, flexible, and lightweight sheet image scanner," in *IEDM Tech. Dig.*, Dec. 2004, pp. 580–581.

[20] H. Kawaguchi, S. Iba, Y. Kato, T. Sekitani, T. Someya, and T. Sakurai, "A sheet-type scanner based on a 3D-Stacked organic-transistor circuit using double word-line and bit-line structure," in *Proc. ISSCC*, Feb. 2005, pp. 365–368.

[21] Y. Kato, S. Iba, R. Teramoto, T. Sekitani, T. Someya, H. Kawaguchi, and T. Sakurai, "High mobility of pentacene field-effect transistors with polyimide gate dielectric layers," *Appl. Phys. Lett.*, vol. 84, pp. 3789–3791, May 2004.

[22] H. Klauk, M. Halik, U. Zschieschang, G. Schmid, W. Radlik, and W. Weber, "High-Mobility polymer gate dielectric pentacene thin film transistors," *J. Appl. Phys.*, vol. 92, pp. 5259–5263, Nov. 2002.

[23] S. F. Nelson, Y.-Y. Lin, D. J. Gundlach, and T. N. Jackson, "Temperature-Independent transport in high-mobility pentacene transistors," *Appl. Phys. Lett.*, vol. 72, pp. 1854–1856, Apr. 1998.

[24] T. Sekitani, S. Iba, Y. Kato, and T. Someya, "Pentacene field-effect transistors on plastic films operating at high temperature above 100 °C," *Appl. Phys. Lett.*, vol. 85, pp. 3902–3904, Oct. 2004.

Takao Someya (M'03) received the Ph.D. degree in electrical engineering from the University of Tokyo, Tokyo, Japan, in 1997.

In 1997, he joined Institute of Industrial Science (IIS), University of Tokyo, as a Research Associate and was appointed Lecturer of the Research Center for Advanced Science and Technology (RCAST), University of Tokyo, in 1998, and an Associate Professor of RCAST in 2002. From 2001 to 2003, he worked for the Nanocenter (NSEC) of Columbia University, New York, and Bell Labs, Lucent Technologies, as a Visiting Scholar. Since 2003, he has been an Associate Professor of the Department of Applied Physics and Quantum-Phase Electronics Center, University of Tokyo. His current research interests include organic transistors, flexible electronics, plastic integrated circuits, large-area sensors, and plastic actuators.
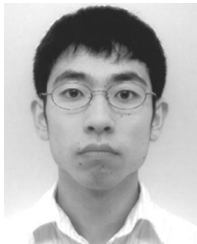
Dr. Someya is a member of the IEEE Electron Devices Society, the Materials Research Society (MRS), and the Japanese Society of Applied Physics.

Tsuyoshi Sekitani was born in Yamaguchi, Japan, in 1977. He received the B.S. degree from Osaka University, Osaka, Japan, and the Ph.D. degree in applied physics from the University of Tokyo, Japan, in 1999 and 2003, respectively.

From 1999 to 2003, he was with the Institute for Solid State Physics (ISSP), University of Tokyo, where he developed measurement techniques in magnetic fields up to 600 T and studied the solid-state physics of condensed matter, especially in high-Tc superconductors. Since 2003, he has been a Research Associate of the Quantum-Phase Electronics Center, University of Tokyo. His current object of physics research is organic semiconductors and organic-FET devices.

Dr. Sekitani is a member of the American Physical Society (APS), the Materials Research Society (MRS), the Physical Society of Japan, and the Japanese Society of Applied Physics.

Yusaku Kato (S'05) was born in Tokyo, Japan, in 1981. He received the B.S. degree in applied physics from the University of Tokyo, in 2004 where he is currently pursuing the M.S. degree in applied physics.
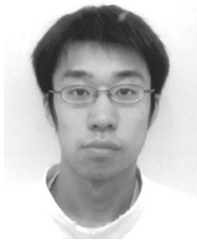
He is currently involved in the development of the new large-area integrated devices that are composed of organic transistors and other functional elements.

Mr. Kato is a member of the Materials Research Society (MRS) and the Japanese Society of Applied Physics.

Hiroshi Kawaguchi (M'98) was born in Kobe, Japan, in 1968. He received the B.S. and M.S. degrees in electronic engineering from Chiba University, Chiba, Japan, in 1991 and 1993, respectively.

He joined Konami Corporation, Japan, in 1993, where he developed arcade entertainment systems. He moved to the Institute of Industrial Science, University of Tokyo, Tokyo, Japan, in 1996 as a Technical Associate, and he is currently a Research Associate. His research interests include low-voltage VLSI designs, low-power hardware systems, wireless circuits, and organic-transistor circuits.

Mr. Kawaguchi is a member of the Association for Computing Machinery (ACM).

Shingo Iba was born in Toyama, Japan, in 1980. He received the B.S. degree in applied physics from the School of Engineering, the University of Tokyo, Tokyo, Japan, in 2004, where he is currently pursuing a graduate debree in organic transistors with double-gate structures for large-area electronic applications.

Mr. Iba is a student member of the Materials Research Society (MRS), and the Japanese Society of Applied Physics.

Takayasu Sakurai (S'77–M'78–SM'01–F'03) received the Ph.D. degree in electrical engineering from the University of Tokyo, Tokyo, Japan, in 1981.

In 1981, he joined Toshiba Corporation, where he designed CMOS DRAM, SRAM, RISC processors, DSPs, and SoC solutions. He has worked extensively on interconnect delay and capacitance modeling known as the Sakurai model and alpha power-law MOS model. From 1988 to 1990, he was a Visiting Researcher at the University of California at Berkeley, where he conducted research in the field of VLSI CAD. Since 1996, he has been a Professor at the University of Tokyo, working on low-power high-speed VLSI, memory design, interconnects, and wireless systems. He has published more than 400 technical papers including 70 invited papers and several books, and has filed more than 100 patents. He is also a consultant to U.S. startup companies.

Dr. Sakurai served as a Conference Chair for IEEE/JSAP Symposium on VLSI Circuits, and IEEE ICICDT, a Vice Chair for ACM/IEEE Asia and South Pacific DAC, and a program committee member for IEEE International Solid-State Circuits Conference, IEEE Custom Integrated Circuits Conference, ACM/IEEE Design Automation Conference, ACM/IEEE International Conference on CAD, ACM FPGA workshop, ACM/IEEE International Symposium on Low-Power Electronics and Design, ACM/IEEE International Workshop on Timing Issues, and other international conferences. He was a plenary speaker for the 2003 ISSCC. He is an elected AdCom member for the IEEE Solid-State Circuits Society and an IEEE Circuits and Systems Society Distinguished Lecturer.

Yoshiaki Noguchi was born in Kanagawa, Japan, in 1983. He received the B.S. degree in applied physics from the University of Tokyo, Tokyo, Japan, in 2005, where he is currently pursuing the graduate degree.

His research interests include organic transistors, large-area electronics, and printed electrical devices.

Mr. Noguchi is a student member of the Japanese Society of Applied Physics.